

# **Investigations into the Effect of Standardized Stress Rates on the Strength and the Deformation Behaviour of a Crystalline Rock Material**

**J. C. Schneider**

*Karlsruhe Institute of Technology, Institute of Soil Mechanics and Rock Mechanics, Karlsruhe, Germany  
jens.schneider@kit.edu*

**H. H. Stutz**

*Karlsruhe Institute of Technology, Institute of Soil Mechanics and Rock Mechanics, Karlsruhe, Germany*

## **Abstract**

Rock and rock mass exhibit time-dependent material behaviour, e.g. mechanical properties change with the load rate. The mechanical properties of rocks are generally described by using simplified modelling approaches. For rock engineering parameters must be determined in laboratory tests. The most common parameters for intact rock are the Young's modulus, Poisson's ratio and the uniaxial strength. The test to determine these values is the uniaxial compression test. This test has been regulated several times by various institutions. The standards differ in detail regarding the test conditions, e.g. load rate. However, all recommendations seldom account for time-dependency to evaluate and determine the most commonly used parameters. In order to study time dependence, a comprehensive test programme was carried out using a homogeneous crystalline rock material. For the uniaxial tests, different stress rates were used, and their effects were examined. The specimens were equipped with a local strain measurement set-up and the results are analysed with respect to the development of the strength and deformation behaviour. An evaluation of the stress thresholds of the different tests is added. The results show that specimen failure is initiated by crack growth. The various tests indicate that fracturing processes are time-dependent, making specimen failure rate-dependent as well.

## **Keywords**

Crystalline rock, uniaxial strength, rock testing, stress thresholds, rate-dependency

## 1 Introduction

The properties of rock are time-dependent; in other words, they change over time, indicating rate-dependence. However, parameters such as uniaxial compressive strength (UCS,  $\sigma_u$ ), Young's modulus ( $E$ ), and Poisson's ratio ( $\nu$ ) are often used in engineering. Usually the major assumption is that these parameters are constants. The  $\sigma_u$ ,  $E$ , and  $\nu$  are determined through the uniaxial compression test (UCT), which is regularised by various standards. These standards and recommendations differ in the suggested loading rates and allow different control parameters such as stress or deformation control. When analysing the recommendations, the lack of clear guidelines for considering the time or rate-dependency of rock properties becomes evident. This inexactness can affect the comparability of the resulting parameter values and their reliability. The test results presented demonstrate the range of achievable parameter values for a specific granite, tested according to various standards at different stress rates. Additionally, the rate-dependency of stress thresholds is examined.

## 2 Uniaxial Compression Testing in Rock Mechanics

### 2.1 Standards and Recommendations

Various institutions have developed their own standards and suggested methods for the uniaxial compression test. In this contribution, three guidelines will be examined (those of the International Society of Rock Mechanics (ISRM) (Bieniawski ZT and Bernede MJ 1979), the German Geotechnical Society (DGGT) (Mutschler T 2004) and the ASTM International (ASTM) (ASTM International 2023). Among other aspects, these recommendations regulate specimen preparation, testing procedure and provide information on evaluation. The recommendations differ with regard to the load control and optional load rates. The ISRM suggest conducting tests with constant force increase. The DGGT and the ASTM suggest both force-controlled and strain-controlled tests. In this contribution the focus is on the effect of the rate in UCT with force control (stress rate). All other test conditions, such as specimen preparation, are selected in such a way that all the mentioned standards are equally fulfilled. The different stress rates suggested by the standards are summarised in Table 1. The table also includes additional time requirements for the test duration of the standards.

Table 1: Suggested stress rates and time requirements for test duration of different standards

Standard	Min Stress rate [MPa/min]	Max stress rate [MPa/min]	Time requirements [min]
ISRM	30	60	5 to 10
DGGT	2	10	>5
ASTM	30	60	2 to 15

### 2.2 Parameter Definitions

The standards contain several options on how to evaluate the measured test data. The methods used in this contribution are introduced in this section. It should be emphasized that the selected methods comply with all the mentioned standards.

#### Stress, Strain and Strength

All three standards define the applied stress as the actual loaded force related to the cross-sectional area of the unloaded specimen, see Eq. 1.

$$\sigma = \frac{P}{A_0} \quad (1)$$

Where  $\sigma$  stress  
 $P$  load  
 $A_0$  cross sectional area of unloaded specimen

The uniaxial strength ( $\sigma_u$ ) of the specimen is considered to be the maximum stress calculated from the maximum load that the test specimen can withstand before failure occurs. Failure is characterised by a significant change in material behaviour. In case of brittle materials as crystalline rocks, this can result in the shattering of the specimen. Neither of the standards prescribe a specific failure mechanism nor exclude a specific fracture pattern.

The axial strain and lateral strain can be calculated using Eq. 2 and Eq. 3. The ISRM also proposes determining the volumetric strain from these strains using Eq. 4.

$$\varepsilon_a = \frac{\Delta l}{l_0} \quad (2)$$

$$\varepsilon_l = \frac{\Delta C}{C_0} \quad (3)$$

$$\varepsilon_v = \varepsilon_a + 2\varepsilon_l \quad (4)$$

Where  $\varepsilon_a$  axial strain  
 $\Delta l$  change in axial gauge length  
 $l_0$  original undeformed axial gauge length  
 $\varepsilon_l$  lateral strain  
 $\Delta C$  change in circumference  
 $C_0$  original specimen circumference  
 $\varepsilon_v$  volumetric strain

### Young's Modulus

The three standards suggest various methods for determining Young's modulus ( $E$ ). The calculation is carried out according to Eq. 5.

$$E = \frac{\Delta \sigma}{\Delta \varepsilon_a} \quad (5)$$

Where  $E$  axial Young's modulus  
 $\Delta \sigma$  change in stress  
 $\Delta \varepsilon_a$  change in axial strain

In this study, the method of the average modulus of the more-or-less straight-line portion of the axial stress-axial strain curve is applied. According to the DGGT the stress-strain data pairs corresponding to 40% and 60% of the maximum stress are used to determine this portion ( $E_{(40-60)}$ ).

### Possion's Ratio

In accordance with the recommendations, the range between 40 % and 60 % of the maximum stress was also chosen to determine the Poisson's ratio ( $\nu_{(40-60)}$ ). Generally, the calculation is carried out according to the Eq. 6.

$$\nu = -\frac{\Delta \varepsilon_l}{\Delta \varepsilon_a} \quad (6)$$

Where:  $\nu$  Poisson's ratio  
 $\Delta \varepsilon_l$  change in lateral strain

## 2.3 Stress Thresholds and Characteristic Regions

An analysis that goes beyond the three recommendations concerns the so-called stress thresholds. These thresholds are stress values that define characteristic regions in the stress-strain diagram of a compression test, as shown in Fig. 1. The definition of the stress thresholds goes back to extensive research published since the middle of the last century. An overview can be found in Nicksiar and Martin (2012), Zhang et al. (2020) or Zhang et al. (2023).

### Region I and Crack Closure Threshold

Region I of the stress-strain curve of crystalline rock describes the initial area in which the stiffness of the specimen increases until it reaches a nearly constant value. The variable stiffness is explained by the closure of pre-existing damage, such as micro-cracks, in the rock under applied load. As these cracks close, the material approaches the stiffness of an almost non-damaged rock. The region is designated as 'Crack Closure', and the stress where microcracks are fully closed is called the Crack Closure Stress ( $\sigma_{CC}$ ) of the Crack Closure Threshold (CC). Beyond this threshold, the material behaviour transitions into Region II.

### Region II and Crack Initiation Threshold

Region II is characterised by an almost linear development in the axial and lateral strain and is often designated as the elastic region. Region II ends at the Crack Initiation Threshold (CI) by the Crack Initiation Stress ( $\sigma_{CI}$ ). This is considered to be the beginning of the development of new cracks in the rock due to the increase of the load. It therefore makes sense to also evaluate the Young's modulus and the Poisson's ratio in this region ( $E_{II}$ ,  $\nu_{II}$ ). The calculation is analogous to the description in 2.2 by

using Eq. 5 and Eq 6. The corresponding stress and strain values of CC and CI are used to calculate the average slope.

### Region III and Crack Damage Threshold

The third region is the portion of the stress-strain curve associated with stable crack growth. With increasing stress, the number and extent of microcracks increases. This is indicated by a decreasing stiffness. Lateral strain shows this deviation more clearly than axial strain, which can be explained by the vertical orientation of new cracks. The development of the axial and lateral strain results in a maximum of the volumetric strain. This point characterises the ‘crack damage threshold’ (CD) and the corresponding stress is the crack damage stress ( $\sigma_{CD}$ ). CD is interpreted as the beginning of unstable crack growth. The maximum of the volumetric strain is also the point at which the volumetric strain changes from a contraction to a dilation within the compression. The term ‘onset of pre-peak dilation’ is also sometimes used for CD.

### Region IV and Peak Stress

If the stress exceeds the CD, it is assumed that the growing microcracks in the rock start to open and coalesce. This region is called the region of unstable crack growth. This means that even if the stress is not increased further but kept constant, the growth of microcracks continues and the rock fails almost immediately. Failure is reached at the peak threshold and is synonymous with UCS ( $\sigma_u$ ). If there is no turning point in the volume strain before the peak value of the stress is reached, CD and UCS are considered to be the same.

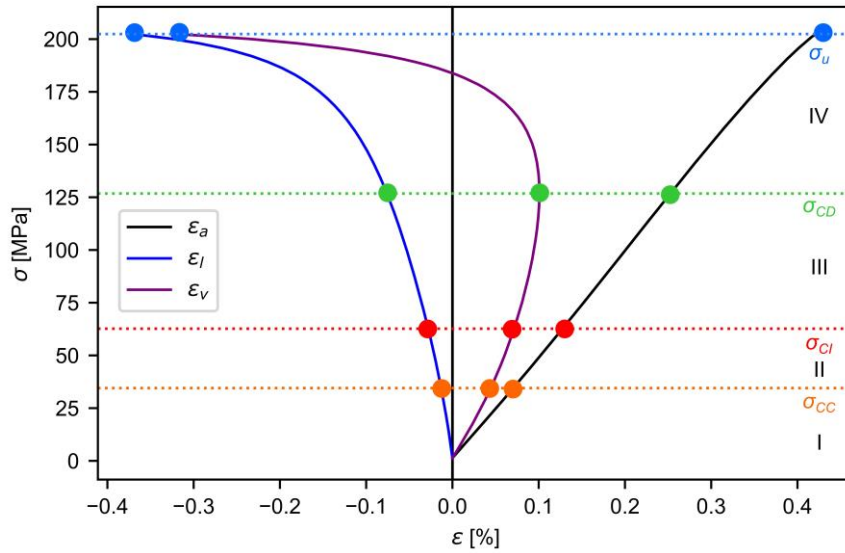


Fig. 1: Example of a Stress strain diagram of a tested specimen with the stress thresholds and characteristic regions.

## 3 Comparative Test Series

A total of 30 UCT were carried out and tested using six different stress rates. The ranges of the recommended rates of the DGGT, ASTM and ISRM were considered in the tests by using rates of 2, 10, 30 and 60 MPa/min. In addition, a faster (120 MPa/min) and a slower rate (1 MPa/min) were added to the test programme.

### 3.1 Rock Material and Specimen Description

For the comparative study, a natural rock material with properties as homogeneous as possible was chosen to ensure the production of comparable specimens. The selected material was a fine-crystalline granite sourced from a quarry in Alpalhão, Nisa, Portalegre, Portugal. In this quarry, blasting is avoided to minimize pre-damage to the rock. Instead, the blocks are sawn from the rock mass according to the specific requirement. The test specimens were produced from a granite block by sawing, drilling and grinding. A specimen diameter of  $d = 70$  mm was selected, and the length-to-diameter ratio ( $L/d$ ) was approximately 2.25. The parallelism tolerance and the lateral surfaces of the specimens conform to the applicable ranges of the mentioned standards. In order to keep the test results as comparable as possible, preliminary tests were carried out on the specimens to

verify the assumed homogeneity. In these tests, the density was analysed and the ultrasonic velocity of the specimens was determined using ultrasonic p-wave travel-time measurement. The analysis is supplemented by the determination of the water content after the actual UCTs. The results of this homogeneity control are summarised in the box plots in Fig. 2.

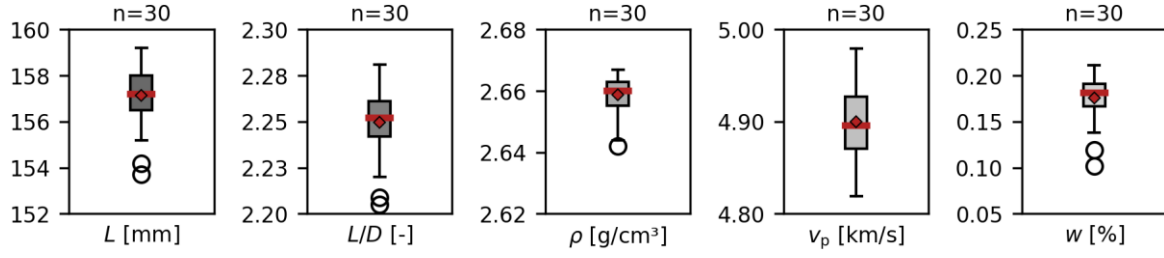


Fig. 2 Box plots of the homogeneity verifying tests. From left to right: length ( $L$ ), length/diameter-ratio ( $L/D$ ), density ( $\rho$ ), p-wave-velocity ( $v_p$ ) and water content ( $w$ ). The red diamond indicates the mean, the horizontal line the median. The box spans for the middle 50% of the analysed parameters (interquartile range), and the whiskers show the range of the data excluding outliers. Outliers are values that lie more than 1.5 times the interquartile range from the box and are shown as individual circle outside the whiskers. The number of tests analysed per box plot is given above the chart ( $n$ ).

### 3.2 Experimental Set-Up

The UCTs were carried out with a servo-hydraulic press. The system has a capacity of 5000 kN axial force and a load cell with an accuracy  $\pm 1\%$  between 50 kN to 5000 kN. The press includes a spherical seat on the top plate and is confirm to the mentioned recommendations. The axial and lateral strains were recorded with a local strain measurement. For this purpose, two strain gauges were attached to the specimen in horizontal and vertical direction. They were temperature-compensated using a Wheatstone bridge and a six-wire circuit, along with a reference rock specimen.

### 3.3 Methods for Threshold Determination

The UCS and the CD are clearly defined and simple to identify. However, CI and CC are more challenging to specify. Several methods have been proposed, but some require subjective assessments, making them challenging to automate or reproduce. A comparative study by Zang et al. (2023), has evaluated different methods and provides recommendations. Following these recommendations, this contribution uses the Lateral Strain Response (LSR) method (Nicksiar and Martin 2012) to evaluate  $\sigma_{CI}$  and the Compression Coefficient Response (CCR) method (Zhang et al. 2020) to determine  $\sigma_{CC}$ . Both methods rely on stress-strain measurements and are considered to be objective.

#### The Lateral Strain Response Method

The LSR method uses the lateral strain response observed prior to the onset of unstable crack growth ( $\sigma_{CD}$ ) to derive  $\sigma_{CI}$ . Following this method, the relationship between axial stress and lateral strain within the range from zero to the  $\sigma_{CD}$  is established. A reference line is constructed by connecting two points on the curve: one corresponding to zero stress and the other to  $\sigma_{CD}$ . Next, the horizontal differences between the lateral strain on the curve and the corresponding lateral strain on the reference line for the same load are computed. The  $\sigma_{CI}$  is identified as the stress level where the lateral strain difference reaches its maximum value.

#### Compression Coefficient Response Method

Zhang and Tang (2020) introduced the compression coefficient ( $\omega$ ), which characterizes the deformation properties of rock under compression before the formation of secondary microcracks. It is defined as Eq. 7, where  $\varepsilon_1$  represents the axial strain, and  $\varepsilon_1^{CI}$  denotes the axial strain at the CI.

$$\omega = \frac{\varepsilon_1^{CI} - \varepsilon_1}{\varepsilon_1^{CI}} \quad (7)$$

Where:  $\omega$                       compression coefficient  
 $\varepsilon_1^{CI}$                       axial strain at  $\sigma_{CI}$

On this basis, the CCR method identifies CC. The method involves obtaining the axial strain curve for stresses ranging from zero to the  $\sigma_{CI}$  and calculating the compression coefficients to determine the relationship between axial stress and the compression coefficient. A reference line is drawn between the points corresponding to zero and the  $\sigma_{CI}$  stress. The compression coefficient difference, defined as

the horizontal deviation between the reference value and the measured compression coefficient, is then calculated. The  $\sigma_{CC}$  is identified as the stress level where the compression coefficient difference reaches its maximum value.

## 4 Results

### 4.1 UCS and Stress Thresholds

The effects of the different rates on the stress thresholds are shown in Fig. 3 as box plots. Each of the thresholds has its own box.

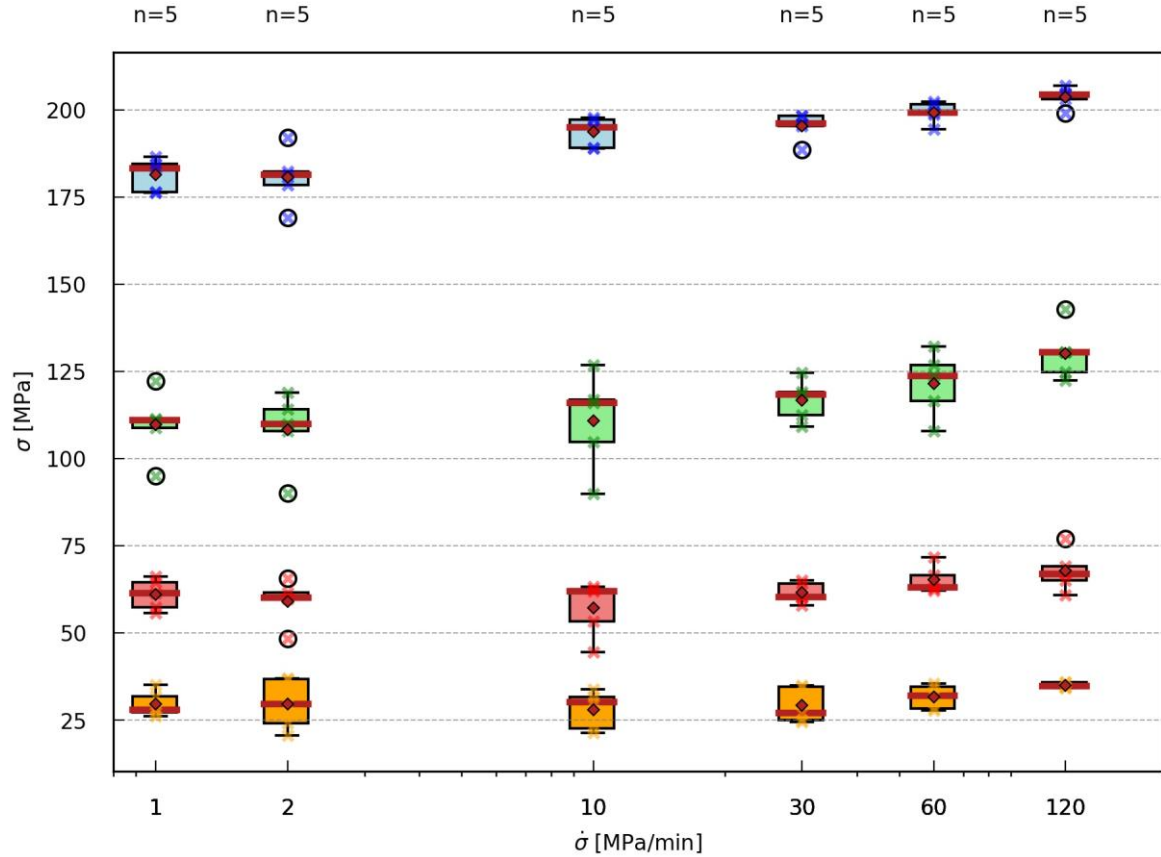


Fig. 3: Box plots of the stress thresholds of different stress rates.  $\sigma_u$  in blue,  $\sigma_{CD}$  in green,  $\sigma_{CI}$  in red and  $\sigma_{CC}$  in yellow. The red diamond indicates the mean, the horizontal line the median. The box spans for the middle 50% of the analysed parameters (interquartile range), and the whiskers show the range of the data excluding outliers. Outliers are values that lie more than 1.5 times the interquartile range from the box and are shown as individual circle outside the whiskers. The number of tests analysed per box plot is given above the chart (n).

The  $\sigma_u$  of the individual tests of the same rates varies only slightly. With increasing rates, an increase in the mean and median values can be observed. The mean and the median result of the slowest rate is an exception of this trend. These results are almost the same as the results of the tests of 2 MPa/min but are slightly higher.

The difference between the lowest (180.67 MPa) and highest mean value (203.67 MPa) is approximately 23 MPa, which corresponds to an increase of 12.8 %. The fluctuations for the  $\sigma_{CD}$  values, are greater than for the  $\sigma_u$  values. As the rate increases, both the mean and median values increase in a similar manner to the  $\sigma_u$  values. Again, the mean of the slowest rate is an exception of this trend. The  $\sigma_{CC}$  values fluctuate similarly to the  $\sigma_{CI}$  values and both do not show a rate-dependency.

### 4.2 Deformation Parameters

Fig. 4 shows the determined deformation parameters  $E_{(40-60)}$  and  $\nu_{(40-60)}$  for the achieved stress range of 40-60 % of  $\sigma_u$ . In addition, the respective parameters determined for the region II are presented. Despite the high demands on the materials, the  $E$  values show relatively large fluctuations. No rate-dependent trend can be identified.

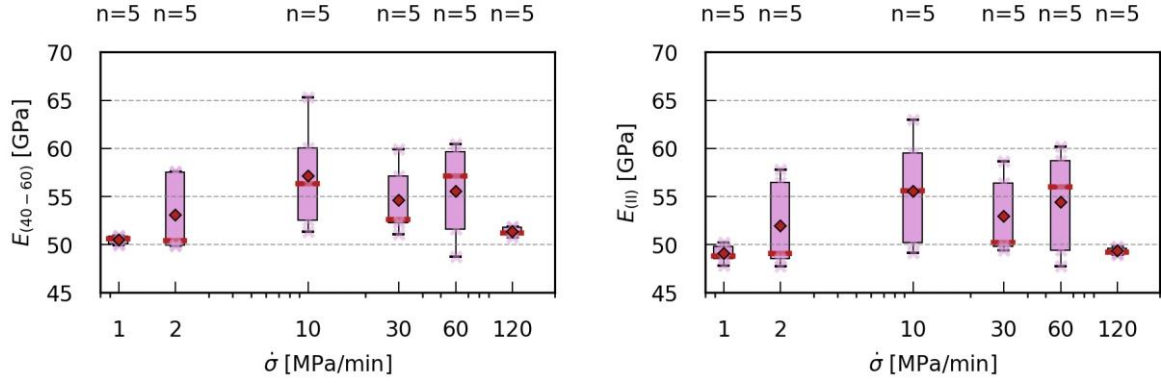


Fig. 4: Left: box plots of the Young's modulus determined between 40-60% of  $\sigma_u$  ( $E_{(40-60)}$ ) for different stress rates; right: Box plots of the Young's modulus determined in Region II ( $E_{(II)}$ ) for different stress rates. The red diamond indicates the mean, the horizontal line the median. The box spans for the middle 50% of the analysed parameters (interquartile range), and the whiskers show the range of the data excluding outliers. Outliers are values that lie more than 1.5 times the interquartile range from the box and are shown as individual circle outside the whiskers. The number of tests analysed per box plot is given above the chart (n).

The results of the Poisson's ratios are shown in Fig 5. There are also major fluctuations here, and the mean values do not indicate a clear trend. The range of fluctuation of the parameters determined in region II is significantly smaller. No rate-dependency is recognisable here.

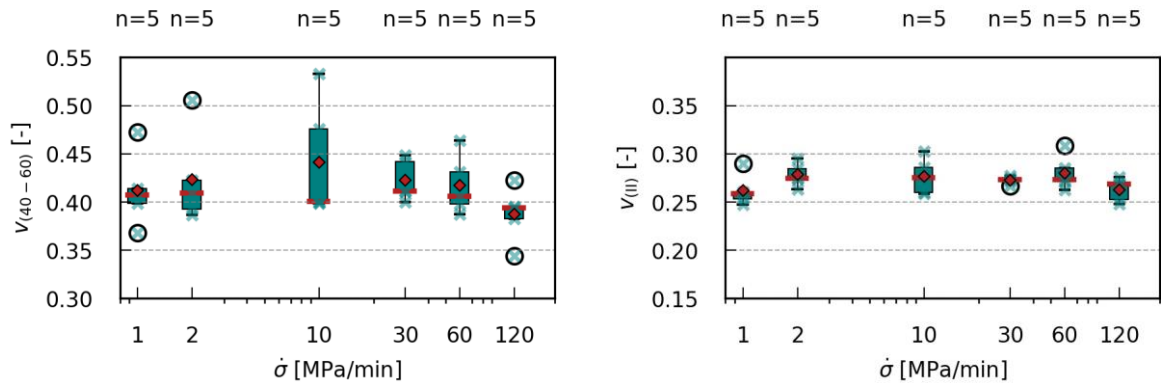


Fig. 5: Left: box plots of the Poisson's ratio determined between 40-60% of  $\sigma_u$  ( $\nu_{(40-60)}$ ) for different stress rates; right: box plots of the Poisson's ratio determined in region II ( $\nu_{(II)}$ ) for different stress rates. The red diamond indicates the mean, the horizontal line the median. The box spans for the middle 50% of the analysed parameters (interquartile range), and the whiskers show the range of the data excluding outliers. Outliers are values that lie more than 1.5 times the interquartile range from the box and are shown as individual circle outside the whiskers. The number of tests analysed per box plot is given above the chart (n).

## 5 Discussion and Summary

For this contribution, a test programme with 30 uniaxial compression tests was carried out. In this context, various stress rates were tested. These correspond to the different rates as suggested or prescribed by three different standards. The UCS results show a trend, with mean values increasing at higher rates. Only the results of the tests of the slowest rate do not fit in this trend. The UCS values are based solely on force measurements relative to the initial cross-sectional area of the specimens, without considering deformation data. Therefore, this trend appears qualitatively robust, even with a relatively small number of experiments. To confirm the trend and determine whether the divergence at the slowest rate is due to natural scattering of the rock properties, additional test will be conducted for all of the six rates. Evaluating stress thresholds, involves both force and deformation measurements. The latter are more prone to errors due to their dependence on the accuracy of the strain gauge attachment. Even slight deviations from perfect vertical or horizontal alignment can affect the measurements, especially for the calculated volumetric strain, which is based on two strain measurements. Despite variability in individual results, the overall experiment series remains



interpretable. The trend of the  $\sigma_u$  is similar for the  $\sigma_{CD}$ . Here, the mean values also rise with each increase in the rate. Again, the results of the slowest rate are an exception to the trend and more tests are needed to clarify this observation.  $\sigma_{CI}$  and  $\sigma_{CC}$ , appear to be rate independent. When analysing the deformation parameters, there is no obvious trend for the  $E_{(40-60)}$  and  $E_{(II)}$ . The ranges are slightly different but both do not show a rate-dependency. The  $\nu_{(40-60)}$  results do not exhibit a clear trend. The scatter is too large to identify any rate dependency. For the  $\nu_{(II)}$ , the values determined are more uniform and significantly smaller compared to  $\nu_{(40-60)}$ . This is consistent with the assumption that the thresholds  $\sigma_{CC}$  and  $\sigma_{CI}$  limit the elastic portion of the material behaviour where no cracks grow. It is generally accepted that the first cracks during uniaxial compression testing begins to grow at the tips of randomly oriented pre-existing microcracks. From there, the cracks develop along a curved path until they align parallel to the direction of the major principal stress and open while the pre-existing cracks close. This has been observed by various authors for different materials and can be found, for example, in Eberhardt et al. 1998. Therefore, the lateral strain is increasing more than the axial strain. The mean values of  $\nu_{(II)}$  show a small scatter and no rate dependency. This aligns with the hypothesis that, in this region, no cracks propagate, so the material is unaffected by time-dependent or rate-dependent crack growth.

The results of the test series do prove that there is an undeniable influence of the selection of test rate on the UCS. The material already shows a clear drop in  $\sigma_u$  within the different suggested rates whereby the test duration is extended from minutes to hours. It is clear, that the processes of crack growth are time-dependent, which is already evident from the changes in tested rates. However, the determined rate-dependencies are not yet sufficient to draw conclusions about the actual time-dependent behaviour of the material for longer timespans. The long-time behaviour must be clarified by other tests like creep tests or time-to-failure tests. When designing the test programmes for civil engineering projects to determine parameters for modelling, some consideration should be given to which rate corresponds to the research question. If the strengths of different rocks are to be compared, the tests should be done in the same load control and rate to ensure comparability. The time required to reach the UCS logically increases with a reduction in the rates. In practice, quick results are often preferred, which can lead to faster tests that may overestimate the material strength.

## References

- ASTM International (2023) Standard test methods for compressive strength and elastic moduli of intact rock core specimens under varying states of stress and temperatures. ASTM International D 7012 -23: 1-10
- Bieniawski ZT, Bernede MJ (1979) Suggested methods for determining the uniaxial compressive strength and deformability of rock materials. International Journal of Rock Mechanics and Mining Sciences & Geomechanics Abstracts, Volume 16, Issue 2, 137-140
- Eberhardt E., Stead S., Stimpson B. Read R.S. (1998) Identifying crack initiation and propagation thresholds in brittle rock. Canadian Geotechnical Journal 35(2):222-233. DOI: 10.1139/cgj-35-2-222
- Nicksiar M, Martin CD (2012) Evaluation of Methods for Determining Crack Initiation in Compression Tests on Low-Porosity Rocks. Rock Mechanics and Rock Engineering 45:607–617. DOI 10.1007/s00603-012-0221-6
- Mutschler T (2004) Neufassung der Empfehlung Nr. 1 des Arbeitskreises „Versuchstechnik Fels“ der Deutschen Gesellschaft für Geotechnik e. V.: Einaxiale Druckversuche an zylindrischen Gesteinsprüfkörpern. Bautechnik 81, Heft 10: 825-834
- Zhang ZH, Tang CA (2020) A Novel Method for Determining the Crack Closure Stress of Brittle Rocks Subjected to Compression. Rock Mechanics and Rock Engineering 53, 4279–4287. <https://doi.org/10.1007/s00603-020-02156-6>
- Zhang ZH, Liang Z, Tang CA, Kishida K (2023) A Comparative Study of Current Methods for Determining Stress Thresholds of Rock Subjected to Compression. Rock Mechanics and Rock Engineering 56:7795–7818. <https://doi.org/10.1007/s00603-023-03480-3>